Structural foundations of resting-state and task-based functional connectivity in the human brain

Ann M. Hermundstad[a,b,1], Danielle S. Bassett[a,c], Kevin S. Brown[a,d,e], Elissa M. Aminoff[f], David Clewett[g], Scott Freeman[h], Amy Frithsen[i], Arianne Johnson[i], Christine M. Tipper[j], Michael B. Miller[i], Scott T. Grafton[i], and Jean M. Carlson[a]

[a]Department of Physics, University of California, Santa Barbara, CA 93106; [b]Department of Physics and Astronomy, University of Pennsylvania, Philadelphia, PA, 19104; [c]Sage Center for the Study of the Mind, University of California, Santa Barbara, CA 93106; [d]Department of Chemical, Materials, and Biomolecular Engineering, University of Connecticut, Storrs, CT 06269; [e]Department of Marine Sciences, University of Connecticut, Groton, CT 06340; [f]Center for the Neural Basis of Cognition, Carnegie Mellon University, Pittsburgh, PA 15213; [g]Neuroscience Graduate Program, University of Southern California, Los Angeles, CA 90089; [h]Department of Psychology, University of California, San Diego, CA 92093; [i]Department of Psychological and Brain Sciences, University of California, Santa Barbara, CA 93106; and [j]Brain and Creativity Institute, University of Southern California, Los Angeles, CA 90089

Edited by Marcus E. Raichle, Washington University in St. Louis, St. Louis, MO, and approved February 28, 2013 (received for review November 21, 2012)

Magnetic resonance imaging enables the noninvasive mapping of both anatomical white matter connectivity and dynamic patterns of neural activity in the human brain. We examine the relationship between the structural properties of white matter streamlines (structural connectivity) and the functional properties of correlations in neural activity (functional connectivity) within 84 healthy human subjects both at rest and during the performance of attention- and memory-demanding tasks. We show that structural properties, including the length, number, and spatial location of white matter streamlines, are indicative of and can be inferred from the strength of resting-state and task-based functional correlations between brain regions. These results, which are both representative of the entire set of subjects and consistently observed within individual subjects, uncover robust links between structural and functional connectivity in the human brain.

cortical networks | diffusion MRI | functional MRI

Human cognitive function is supported by large-scale interactions between different regions of the brain. The anatomical scaffolding that mediates these interactions can be described by a structural connectome that maps the spatial layout of white matter (1). Structural connectivity (SC), defined by the physical properties of these direct anatomical connections, supports the relay of electrical signals between brain regions. Neurophysiological events can similarly be described by a functional connectome that maps coordinated changes in neuronal activity, field potentials, blood flow, or energy consumption (2). Functional connectivity (FC), defined by temporal correlations in such neurophysiological events, reflects the resting-state and task-dependent strengths of correlated activity in different brain regions (3–5). The estimation of structural and functional connectivity from different experimental techniques raises two complementary questions about the quantitative relationships between structural and functional connectomes: (*i*) to what extent can the resting-state and task-dependent strengths of functional correlations between brain regions be inferred from structural connectomes, and (*ii*) to what extent can the physical properties of anatomical connections be inferred from functional connectomes?

Connectomes, whether examined at the neural or systems level, are networks whose structural properties, such as the length and number of connections, can differentially impact functional properties, such as local or global correlations in temporal dynamics. Whereas the length and density of anatomical connections are thought to impact functional processes such as information segregation and integration (6, 7), the extent to which such relationships are robustly observed in the human brain is not well understood. Previous studies have been limited in scope to specific anatomical connections and brain regions, small sample sizes, and resting-state neural activity (8–13) and have consequently left several fundamental questions unanswered. How do variations in structural features, such as the length and number of anatomical connections, differentially contribute to functional correlations? To what extent do these contributions vary across cognitive states to distinguish between resting, task-general, and task-specific FC? Can we distinguish between features that are reflective of underlying organizational principles and those that are potentially predictive of behavior?

We address these questions by combining the specificity of anatomical and functional analysis with the statistical power of 84 subjects measured noninvasively at rest and during the performance of attention- and memory-demanding tasks. SC is estimated from diffusion tensor imaging (DTI) measurements of white matter, whereas FC is estimated from functional magnetic resonance imaging (fMRI) measurements of changes in blood-oxygenation-level-dependent (BOLD) signals (4).

In what follows, we introduce a set of multimodal approaches for isolating relationships between structural and functional connectivity across subjects and brain states. We compare the structural measures of streamline number and length, thought to differentially impact sensory processing (6, 7), with the task-dependent functional measure of BOLD correlation strength, thought to reflect the coordinated control of different brain regions. We show that partitions in these connectivity measures, in combination with the delineation between inter- and intrahemispheric connectivity, enable both the inference of function from structure and the inference of structure from function. We further identify structural measures that distinguish cognitive states, with interhemispheric and local dense intrahemispheric connectivity supporting resting-state function and long-range intrahemispheric connectivity supporting task-driven function. These findings provide insight into the design of the human brain and the constraints imposed by its architecture.

Model

In constructing brain networks, localized brain regions are represented as nodes, and the strengths of structural or functional connectivity between brain regions are represented as weighted, undirected connections between nodes.

We select regions by subdividing the Automated Anatomical Labeling (AAL) Atlas (14) into 600 regions of similar volume. From this set of regions, we compute structural and functional networks for 84 individual subjects (*SI Appendix*).

Author contributions: A.M.H., D.S.B., K.S.B., M.B.M., S.T.G., and J.M.C. designed research; A.M.H. performed research; E.M.A., D.C., S.F., A.F., A.J., C.T., M.B.M., and S.T.G. contributed new reagents/analytic tools; A.M.H., D.S.B., K.S.B., E.M.A., D.C., S.F., and C.T. analyzed data; and A.M.H., D.S.B., K.S.B., S.T.G., and J.M.C. wrote the paper.

The authors declare no conflict of interest.

This article is a PNAS Direct Submission.

[1]To whom correspondence should be addressed. E-mail: annherm@physics.upenn.edu.

This article contains supporting information online at www.pnas.org/lookup/suppl/doi:10.1073/pnas.1219562110/-/DCSupplemental.

Structural brain networks are obtained from DTI measurements via a tractography algorithm used to identify white matter streamlines. For each subject, we compute two measures of SC: the total number N and average length L of streamlines linking two regions. We define a binary number C that specifies the presence or absence of SC, such that $C_{i,j} = 1$ if regions i and j are linked by one or more streamlines, and $C_{i,j} = 0$ otherwise.

Functional brain networks are obtained from fMRI measurements of BOLD time series. Pearson's correlations are computed between scale 2 wavelet coefficients (0.06–0.125Hz) of regional mean time series. For each subject, we compute three measures of FC: the correlation between two time series measured at rest (resting state) and during the performance of attention and facial recognition memory tasks (attention and memory states, respectively). Analysis of a word recognition memory task produced similar results (*SI Appendix*). Given that task-driven changes in FC are small relative to resting-state values (15), we compare the strength of FC measured at rest (rsFC) to that measured in deviations ΔasFC = asFC − rsFC of the attention state (asFC) from rest and in deviations ΔmsFC = msFC − rsFC of the memory state (msFC) from rest. The integration of FC estimates across subjects (see following section) ensures that this approach selects robust, biologically meaningful variation between task-driven and resting-state FC.

In what follows, we perform two complementary analyses to identify structural properties that are indicative of function (SC→FC) and functional properties that are indicative of structure (FC→SC).

Statistical Methods. The brain exhibits both sparse and variable SC, with far fewer anatomical connections than would be expected at random (16) and with patterns of connectivity that vary between individuals (1). Of the possible 179,700 pairings between 600 regions, less than 2% are measured to be anatomically linked within a given subject, whereas even fewer are measured to be consistently linked across subjects. Despite this observed sparsity of structural connections, functional correlations are inherently nonsparse and can persist between regions that have no direct anatomical link (9).

Previous studies have accounted for the nonsparsity of functional correlations by comparing the presence vs. absence of SC within single subjects (9). However, the desire to reliably assess group-level properties requires that we consider the degree to which SC is consistent across subjects. We therefore choose to examine structural and functional connectivity between region pairs that are linked by direct anatomical connections within a large percentage of subjects. Although this approach necessarily restricts our analysis to a subset of functional correlations, the reliable presence of anatomical connections enables us to extend beyond comparisons of present vs. absent connectivity to isolate specific contributions of different structural measures to FC.

Representative vs. Subject-Specific Analyses. In an analogous manner to the construction of subject-specific brain networks for the assessment of subject-level properties, we can assess group-level properties by constructing a "representative brain network" whose connections are weighted by subject-averaged, rather than subject-specific, values of SC and FC. We use the properties of this representative network to select subsets of consistently connected regions pairs that are used in the subsequent analyses of SC→FC and FC→SC. Care must be taken, however, when assessing FC→SC, as the selection of structurally connected region pairs must be performed indirectly using only nonstructural information so as not to bias the analysis (see following subsection).

Our analysis of SC→FC (and analogously FC→SC) can be summarized in the following steps:

i) select subsets of consistently structurally-connected region pairs based on structural (nonstructural) measures
ii) partition subgroups of connections based on similarities in structural (functional) properties
iii) compare functional (structural) properties of subgroups

Note that the two analyses are completely symmetric (such that SC and FC can be everywhere interchanged), with one exception: both subsets of region pairs are selected (albeit by different measures) based on consistency in SC alone.

We perform these analyses first on the representative brain network. We then verify, using the same sets of region pairs subject to the same partitioning, that the observed structure–function relationships are consistently maintained across subject-specific networks. *SI Appendix* contains an extensive treatment of variations in the parameters used for both selecting and partitioning region pairs, with all results being consistent to those reported here. *SI Appendix* additionally verifies, in a manner consistent with ref. 9, that our results are robust to distance-related effects that could arise from spatially autocorrelated measurements of SC and FC.

Notation. In comparing different connectivity measures, we will refer to the average $\langle O \rangle$ and SD $\sigma\langle O \rangle$ of a given measure O. When computed across subjects, we reference the quantity with the subscript s (e.g., $\langle O \rangle_s$), and when computed across connections within a single subject, we reference the quantity with the subscript c (e.g., $\langle O \rangle_c$).

Selecting Consistently Connected Region Pairs. Within a single subject, the presence of nonzero SC is specified by the set of region pairs with $C_{i,j} = 1$. Identifying consistently nonzero SC then requires that we select, via a thresholding process, region pairs with high values of the subject-averaged value $\langle C \rangle_s$, which we term the "consistency in connectivity." For reasons to be discussed shortly, we choose to perform this process indirectly by thresholding quantities that relate to, but are distinct from, $\langle C \rangle_s$. Importantly, the choice of thresholded quantities need not be the same for the analyses of SC→FC and FC→SC so long as the former does not use information about FC and the latter does not use information about SC.

We find that $\langle C \rangle_s$ increases with both the normalized number of streamlines $\overline{N} = \langle N \rangle_s / \sigma_s(N)$ (a purely structural measure) and the inverse interregional distance $1/d$ (a purely geometric measure of Euclidean distance). We impose thresholds $\overline{N}_T = 0.6$ and $1/d_T = 0.1$ mm^{-1} to select two largely overlapping subsets of region pairs for the respective analyses of SC→FC and FC→SC (Fig. 1*A*). Both subsets are similar in size (3,085 vs. 3,079 region pairs, respectively) and average consistency $\langle C \rangle_{s,c}$ (86% vs. 79%, respectively). Note that there is no optimal nonstructural measure for selecting structurally connected region pairs. Although thresholding in $1/d$ inherently favors the selection of short connections, the resulting ability to reliably estimate consistency in connectivity is crucial for the unbiased inference of SC from FC.

Qualitatively similar results can be achieved by selecting region pairs via the direct measure $\langle C \rangle_s$. We choose instead to select region pairs via $\overline{N}$ and $1/d$ because this selection avoids two drawbacks of using $\langle C \rangle_s$ directly: (*i*) $\langle C \rangle_s$ requires information about SC and is therefore less optimal than $1/d$ for the assessment of FC→SC, and (*ii*) $\langle C \rangle_s$ lacks a single-subject correlate that would enable the extension of these methods to single-subject brain networks and is therefore less optimal than $\overline{N}$ for the assessment of SC→FC. Furthermore, because $\overline{N}$ and $1/d$ scale roughly linearly with one another, it is straightforward to tune $\overline{N}_T$ and $1/d_T$ to achieve a desired consistency and subset size while maintaining similar results.

Comparing Partitioned Subgroups of Region Pairs. In the subsequent analyses, we quantify the extent to which subgroups of connections partitioned based on structural (functional) measures show similarities in functional (structural) properties. We compare the properties of partitioned subgroups by evaluating shifts in the complementary cumulative distribution functions (cCDFs) of a given connectivity measure O. The cCDF(O), which measures the probability of finding $O > O^*$ for every value of O^*, enables the simultaneous comparison of different instantiations of the quantity O. When assessing the representative brain network, we report the full cCDF distributions of $\langle O \rangle_s$. When

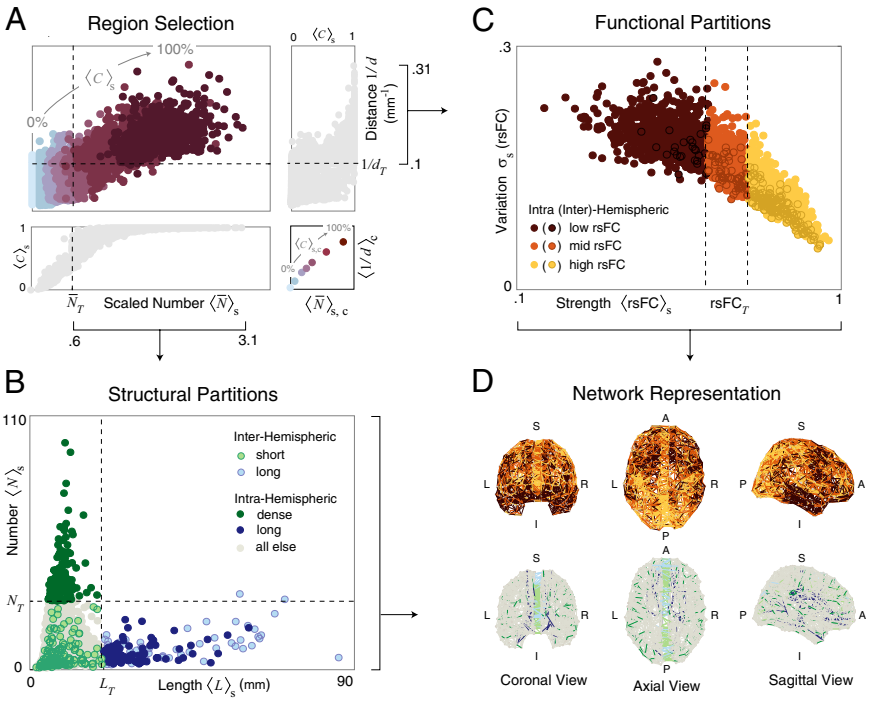

Fig. 1. Constructing and partitioning brain networks. (*A*). Consistency in connectivity $\langle C\rangle_s$ as a function of scaled number $\overline{N}$ and inverse interregional distance $1/d$, with average values $\langle C\rangle_{s,c}$ indicated in the lower right. We impose thresholds $\overline{N}_T$ and $1/d_T$ (dashed lines) to select two largely overlapping subsets of region pairs with high $\langle C\rangle_s$. Regions selected via $\overline{N}_T$ and $1/d_T$ are, respectively, used to infer FC from SC (*B*) and infer SC from FC (*C*). Horizontal and vertical projections show values of $\langle C\rangle_s$ (gray) as a function of $\overline{N}$ and $1/d$. (*B*) Number $\langle N\rangle_s$ vs. length $\langle L\rangle_s$ of streamlines between region pairs selected via $\overline{N}_T$. We apply a length threshold $L_T = 20$ mm and a number threshold $N_T = 30$ (dashed lines), and we further distinguish interhemispheric connections (outlined markers). In combination, these partitions separate four nonoverlapping subgroups, short (light green) and long (light blue) interhemispheric connections and dense (dark green) and long (dark blue) intrahemispheric connections, from the remaining bulk of short, sparse intrahemispheric connections (tan). (*C*) Intersubject variance σ_s(rsFC) decreases for increasing $\langle$rsFC$\rangle_s$ between region pairs selected via $1/d_T$. We apply functional thresholds rsFC_T (dashed lines) to separate low (bottom 33% in brown), intermediate (middle 33% in orange), and high (top 33% in yellow) rsFC, and we further distinguish interhemispheric connections (outlined markers). (*D*) Coronal, axial, and sagittal views of structural and functional subgroups of connections. Gray nodes mark region centers, and straight lines mark curvilinear streamlines in the representative brain.

comparing across subject-specific networks, we report the distribution averages $\langle O\rangle_c$.

Results

Inferring Function from Structure (SC→FC). Structural connections are unevenly distributed between different regions of the brain (17). For example, a significant number of thickly myelinated streamlines is present in the corpus callosum. Similarly, certain brain regions are more densely or distantly interconnected than other regions (18). We investigate the extent to which variations in these structural properties are reflected in the strength of communication between brain regions.

Structural partitions. We separately consider "long" vs. "short" connections, whose lengths are greater and less than a threshold value L_T, and "dense" vs. "sparse" connections, whose numbers are greater and less than a threshold value N_T, where our definition of "density" differs from definitions in which N is scaled by the cross-sectional streamline area. Our choice of thresholds $L_T = 20$ mm and $N_T = 30$, in combination with the delineation between inter- and intrahemispheric connections, defines four nonoverlapping structural subgroups, long and short interhemispheric connections and long and dense intrahemispheric connections, whose properties we compare with the remaining bulk of short, sparse intrahemispheric connections (Fig. 1*B*).

FC of the representative brain. In the resting state, we find striking differences in the strength of FC between regions linked by different types of structural connections (Fig. 2 *A* and *D*). All interhemispheric connections, regardless of length, show strong rsFC. The reduced sensitivity of interhemispheric correlations to variations in connection length could be due to the insulating properties of heavy myelination that help minimize signal decay along interhemispheric streamlines. Dense intrahemispheric connections show similarly strong rsFC, a property that could reflect signal amplification from large numbers of connections (Fig. 2 *E* and *F*). Long intrahemispheric connections, however, show notably weak rsFC despite being of similar length and number to the set of long interhemispheric connections. These observations extend beyond previous findings of increasing rsFC with decreasing interregional distance (9) to identify structural mechanisms that support strong rsFC between nearby inter- vs. intrahemispheric regions.

During task performance, we find that a majority of connections decrease in FC during attention (Fig. 2 *B* and *E*) but increase in FC during memory (Fig. 2 *C* and *F*) relative to their behavior at rest. Interhemispheric and dense intrahemispheric connections, which displayed relatively strong rsFC, show similar changes in both asFC and msFC to the remaining bulk of connections. Long intrahemispheric connections, however, show significant changes in FC between tasks, exhibiting weaker connectivity in the attention state and stronger connectivity in the memory state as compared with the remaining bulk of connections. The magnitude of these changes, which distinguishes attention from memory states, becomes more pronounced when biasing toward longer connections.

Individual variability in FC. The overall strength of FC varies significantly across subjects. Within subject-specific brain networks, however, we find that structural subgroups of connections show qualitatively similar shifts in FC to those observed in the representative brain network. In the resting state, all subjects exhibit strong FC between interhemispheric and densely linked intrahemispheric regions, and they exhibit weak FC between distantly linked intrahemispheric regions (Fig. 2*G*). In attention and memory states, all subjects exhibit similar changes in FC produced by structural subgroups (Fig. 2 *H* and *I*).

Summary of SC→FC. The strong values of rsFC and consistent changes in asFC and msFC exhibited by interhemispheric and dense intrahemispheric connections suggest that these connections support strong resting-state function. In contrast, the weak values of rsFC but large changes in asFC and msFC exhibited by long intrahemispheric connections suggest that these connections support task-dependent changes in attention and memory function and might, in agreement with the implication of long distance connections in motors tasks (19), support more general task-based function.

Inferring Structure from Function (FC→SC). The results of the previous section revealed that the structural features of anatomical connections differentially impact functional correlations between brain regions. As a stronger test of the relationship between SC and FC, we investigate whether functional correlations can similarly be used to infer underlying structural properties.

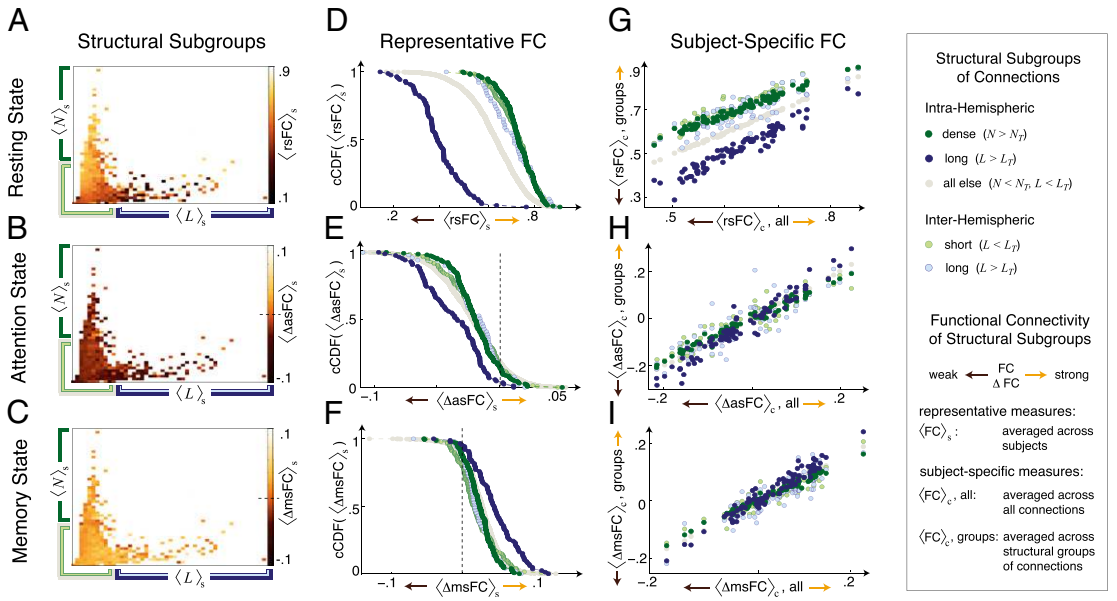

Fig. 2. FC of structural subgroups. Functional measures ⟨rsFC⟩ (*Top*), ⟨ΔasFC⟩ (*Middle*), and ⟨ΔmsFC⟩ (*Bottom*) produced by structural subgroups of connections in representative and subject-specific brain networks. (*A–C*) Density maps of $\langle FC \rangle_s$ vs. $\langle N \rangle_s$ and $\langle L \rangle_s$ in the representative brain, with structural partitions indicated below and to the left of each subfigure. (*A*) In the resting state, we see significant variation in FC across variations in SC. During task performance, we see overall (*B*) suppression during attention and (*C*) activation during memory, with less variation in FC across variations in SC. (*D–F*) cCDFs of $\langle FC \rangle_s$ produced by structural subgroups of connections in the representative brain. (*D*) In the resting state, interhemispheric connections and dense intrahemispheric connections show strong FC, whereas long intrahemispheric connections show weak FC. During task performance, long intrahemispheric connections show larger (*E*) decreases in $\langle FC \rangle_s$ during attention and (*F*) increases in $\langle FC \rangle_s$ during memory compared with the remaining subgroups of connections. (*G–I*) Subject-specific values of $\langle FC \rangle_c$ produced by structural subgroups of connections, where subjects are ordered by overall FC such that each vertical cross-section represents a single subject. (*G*) In the resting state, all subjects show strong $\langle FC \rangle_c$ between interhemispheric and densely-connected intrahemispheric regions, and all subjects show weak $\langle FC \rangle_c$ between distant interhemispheric regions. (*H* and *I*) During task performance, all subjects show similar changes in the strength of $\langle FC \rangle_c$ measured within different structural subgroups.

Functional partitions. Given the pronounced separation in the resting-state properties of structural subgroups, we infer SC from resting-state, rather than task-driven, FC. We apply fixed thresholds $rsFC_T$ to separate weak (bottom 33%), intermediate (middle 33%), and strong (top 33%) rsFC, and we distinguish inter- from intrahemispheric correlations (Fig. 1*C*). Consistent with the previous section, nearly two-thirds of all interhemispheric correlations fall into the strongly correlated subgroup.

SC of the representative brain. We find striking differences in the structural properties of connections that support strong vs. weak correlations (Fig. 3 *A* and *B*), with intrahemispheric region pairs being more densely connected and linked by shorter connections, on average, than interhemispheric region pairs (Fig. 3 *C* and *D*).

Both inter- and intrahemispheric region pairs that show increasingly strong rsFC are linked by an increasingly large number of connections. Whereas increasingly strong interhemispheric FC is further supported by increasing long connections, the separation in the length distributions produced by strongly vs. weakly correlated regions is small and can change across thresholding methods. This finding suggests, in agreement with the previous section, that interhemispheric connection length does not strongly distinguish variations in rsFC.

We additionally find that inconsistent connectivity can alter the apparent distribution of intrahemispheric connection lengths. Correcting for inconsistent connectivity (a process that requires knowledge of SC) reveals that strong rsFC is consistently supported by short intrahemispheric connections (Fig. 3*D*).

Individual variability in SC. We again find significant intersubject variation in the overall number and length of connections, but we find consistent subject-specific shifts in the structural properties that differentially support strong vs. weak correlations.

Individual subjects show strikingly consistent separation in the increasing number of intra- and interhemispheric connections that link strongly vs. weakly correlated regions (Fig. 3*E*). The observed length of these connections, however, is again sensitive to artifacts arising from inconsistent connectivity. If we remove such artifacts, we find that strong intrahemispheric correlations are consistently supported by short connections, whereas interhemispheric regions show reduced separation in the length of connections that support strong vs. weak correlations (Fig. 3*F*).

Summary of FC→SC. The consistent link between connection number and rsFC strength suggests that high numbers of connections facilitate strong FC, regardless of where they are implemented. In comparison, the varied length dependence exhibited by inter- vs. intrahemispheric rsFC suggests that the role of connection length in facilitating strong FC depends on the anatomical properties of the regions linked by these connections.

Discussion

Identifying relationships between structural and functional networks is crucial for understanding the large-scale organization of the human brain. Previous structure-function studies have been limited to specific brain regions, small sample sizes, and resting-state activity (8, 9, 13) for which it is difficult to reliably assess the differential contributions of several structural measures to task-dependent function. In the present study, we develop methods for inferring consistent relationships between structural and functional connectivity across subjects and cognitive states.

Synopsis. This study uncovered several principles of large-scale brain organization. (*i*) Variations in specific structural measures, notably connection length and number, differentially impact FC. (*ii*) Spatial location constrains structure–function relationships, with structurally similar inter- vs. intrahemispheric connections supporting different strengths of functional correlations. (*iii*) These relationships are state-dependent, such that SC differentially impacts resting vs. task-driven cognitive states.

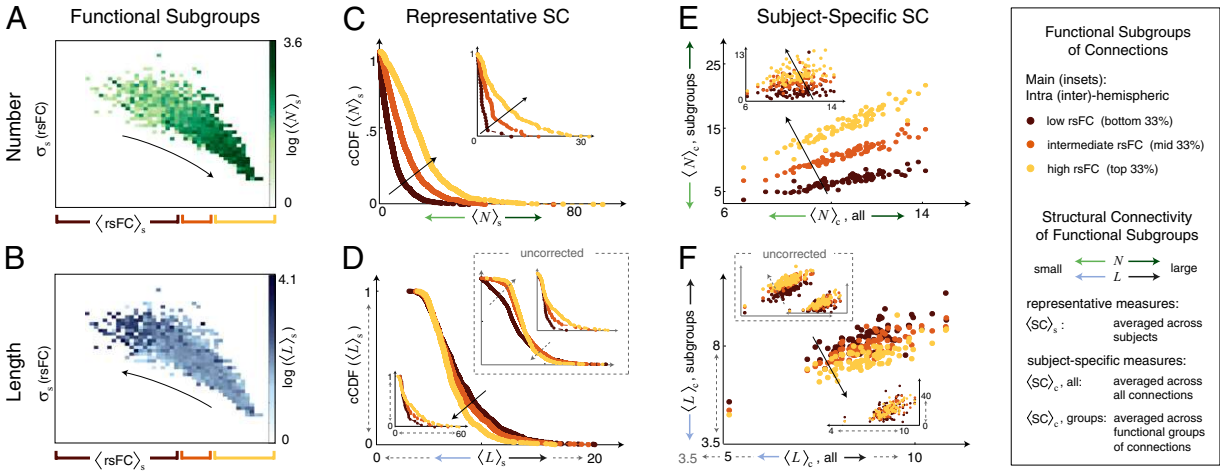

Fig. 3. SC of functional subgroups. Structural measures $\langle N \rangle$ (*Upper*) and $\langle L \rangle$ (*Lower*) produced by functional subgroups of connections within representative and subject-specific brain networks, with the properties of interhemispheric connections shown as insets in subfigures *C–F*. All lengths are given in mm. (*A* and *B*) Density maps of $\log(\langle SC \rangle_s)$ vs. $\langle rsFC \rangle_s$ and $\sigma_s\langle rsFC \rangle$, with functional partitions indicated below each subfigure. We see significant variation in SC across variations in rsFC, with rsFC tending to increase for (*A*) increasing $\langle N \rangle_s$ and (*B*) decreasing $\langle L \rangle_s$. (*C* and *D*) cCDFs of $\langle SC \rangle_s$ produced by structural subgroups of connections in the representative brain. (*C*) Increasingly large numbers of both inter- and intrahemispheric connections support increasingly strong rsFC, and intrahemispheric connections are more numerous, on average, than interhemispheric connections. (*D*) Corrected distributions of $\langle L \rangle_s$ show that increasingly strong correlations are supported by increasingly short intrahemispheric connections and increasingly long interhemispheric connections, with interhemispheric regions linked by longer connections, on average, than intrahemispheric regions. Uncorrected distributions are shown in the dotted *Inset* (with axis scales indicated by dotted lines along the main axes) and reveal that the inclusion of inconsistent connectivity alters the distribution of short lengths. (*E* and *F*) Subject-specific values of $\langle SC \rangle_c$ produced by functional subgroups of connections, where subjects are ordered by overall SC strength such that each vertical cross-section represents a single subject. (*E*) Across subjects, strong rsFC is supported by large numbers of inter- and intrahemispheric connections. (*F*) Corrected values of $\langle L \rangle_c$ show that, across subjects, strong rsFC is consistently supported by short intrahemispheric connections. Uncorrected values (dotted *Inset*) reveal that the inclusion of absent connections reverses the relationships between intrahemispheric connection length and rsFC strength. In both corrected and uncorrected cases, individual subjects show reduced separation in the length of interhemispheric connections that support strong vs. weak correlations.

The combined analyses of FC→SC and SC→FC identify structural properties that consistently support strong resting-state function. We find that large numbers of connections consistently underlie strong rsFC, a result that supports both empirical and computational studies of resting-state activity (9, 20). Connection length distinguishes strong from weak intrahemispheric rsFC but has minimal impact on interhemispheric rsFC.

Analysis of SC→FC further identified structural properties that support task-dependent changes in function. Notably, long-range intrahemispheric connections, which link brain regions important for attention (21, 22) and memory (23, 24) (*SI Appendix*), are found to both support and distinguish between attention and memory states. We find that global changes in FC additionally distinguish between task states, with overall FC increasing during attention but decreasing during memory compared with rest. This result is compatible with findings that default mode and fronto-parietal FC increases in memory relative to rest, with FC between these networks and cingulo-opercular and cerebellar networks increasing with memory load (25).

The observation of structurally mediated FC does not discount previous findings that functional correlations can persist in the absence of direct SC, as is observed in persons with agenesis of the corpus callosum (26), and may be mediated by indirect SC (9). Although these findings have suggested that the inference of SC from FC is impractical (9), we show that such inference is reliable within a subset of region pairs. These results support the utility of BOLD fluctuations not only as a measure of functional correlations but also as a measure of the underlying structural features that support such correlations.

Implications for Development, Aging, and Disease. Changes in resting and task-driven FC have been linked to both development (27, 28) and aging (29, 30). Intriguingly, older adults have been shown to more strongly recruit homologous regions in opposing hemispheres to maintain task performance (31). The resulting patterns of functional compensation rely on the microstructural integrity of the corpus callosum, suggesting that white matter structure constrains adaptive brain function with age (32). Taken with our present findings, greater task-related interhemispheric FC may compensate for age-related declines in the structural properties of the long intrahemispheric connections that we find to support attention and memory processes.

These results provide further insight into the structural mechanisms that could contribute to the altered FC observed in neurological disorders (33, 34). Disruptions to dense connections could affect the topological nodal properties of network hubs, a consequence that has been linked to altered rsFC in diseases such as epilepsy (35). Disruptions to interhemispheric connections could similarly reduce rsFC, as is observed in patients with axonal injury in the corpus callosum (36). As changes in FC have been linked to variability in task performance (37, 38), structural disruptions are further expected to impact behavior across a range of cognitive tasks.

Methodological Considerations. Individual variability in SC may arise in part from the use of an atlas-based, rather than individual surface-based, parcellation of cortical and subcortical brain regions (*SI Appendix*). However, the observed sparsity in individual SC has been shown in previous studies to be highly robust across scanning sessions (16). Furthermore, recent results have indicated that fiber pathways can exhibit abrupt turns that would not be identified by the tractography algorithm used here (18). Such deterministic algorithms can similarly fail to distinguish branching and crossing fiber pathways, a limitation that can bias, for example, interhemispheric SC toward midline structures. The presence of these pathways, which may be better identified via probabilistic tractography algorithms (e.g., ref. 39), warrants further exploration and is expected to strengthen the structure–function relationships observed here.

Whereas the analyses of FC→SC and SC→FC produce consistent results, the latter analysis is more difficult. The difficulty arises in selecting, without knowledge of SC, region pairs that show consistent SC across subjects. Whereas consistent SC can

be achieved by restricting the analysis to small interregional distances, this approach biases against the selection of the task-relevant set of long intrahemispheric connections, hindering the inference of SC from task-driven FC.

The methodological approaches developed here focus on raw measures of direct pairwise connectivity and can therefore be broadly applied to a range of interconnected systems. The application of higher-order connectivity measures such as modularity, clustering, and path length to the present analysis may help bridge the findings of previous studies that have separately assessed structural (8, 16) and functional (19, 40) human brain networks (see ref. 41 for a review). Alternative methods can be used to explicitly model resting-state and task-based neural activity (see, e.g., ref. 42), and such methods may additionally help elucidate the task-dependent features of neural activation patterns that contribute to the structure–function relationships observed here.

Final Remarks. In concluding, we can speculate as to why the brain might be structured in this manner, with many short and few long connections that differentially impact resting vs. task-driven function. Connections are energetically expensive to both maintain and use (43–46), favoring short and sparse over long and dense connectivity. However, few long connections might more efficiently transmit information between distant regions, as is needed during task performance, than do many short connections. Conversely, dense connectivity might enhance the robust properties of default mode function by reducing the potential impact of local disruptions to the structural integrity of white matter streamlines. Finally, an insensitivity of resting-state correlations to variations in connection length could be crucial for functionally binding the two hemispheres, which, although structurally segregated, must support a single cognitive identity.

It remains a challenge for future theoretical, computational, and experimental studies to examine in greater detail the biophysical origins of this organization. The present study lays a strong foundation for such investigations, as it provides insight into the principles that might have constrained the evolution and development of anatomical brain architecture, and it makes specific predictions about the functional implications of degradations to this architecture. Identifying links between anatomical and functional connectivity is crucial for understanding the capabilities of and constraints on human cognitive function.

ACKNOWLEDGMENTS. This work was supported by the David and Lucile Packard Foundation and the Institute for Collaborative Biotechnologies through Contract W911NF-09-D-0001 from the US Army Research Office. D.S.B. was additionally supported by the Errett Fisher Foundation, the Templeton Foundation, and the Sage Center for the Study of the Mind.

1. Sporns O, Tononi G, Kötter R (2005) The human connectome: A structural description of the human brain. *PLOS Comput Biol* 1(4):e42.
2. Lee JH, et al. (2010) Global and local fMRI signals driven by neurons defined optogenetically by type and wiring. *Nature* 465(7299):788–792.
3. Aertsen A, Preissl H (1991) Dynamics of activity and connectivity in physiological neuronal networks. In: Nonlinear Dynamics and Neuronal Networks, Schuster H (ed), VCH Verlag, Weinheim, pp 281–301.
4. Friston KJ (1994) Functional and effective connectivity in neuroimaging: A synthesis. *Hum Brain Mapp* 2:56–78.
5. Friston KJ (2011) Functional and effective connectivity: A review. *Brain Connect* 1(1):13–36.
6. Clavagnier S, Falchier A, Kennedy H (2004) Long-distance feedback projections to area V1: Implications for multisensory integration, spatial awareness, and visual consciousness. *Cogn Affect Behav Neurosci* 4(2):117–126.
7. Tononi G, Sporns O, Edelman GM (1994) A measure for brain complexity: Relating functional segregation and integration in the nervous system. *Proc Natl Acad Sci USA* 91(11):5033–5037.
8. Hagmann P, et al. (2008) Mapping the structural core of human cerebral cortex. *PLoS Biol* 6(7):e159.
9. Honey CJ, et al. (2009) Predicting human resting-state functional connectivity from structural connectivity. *Proc Natl Acad Sci USA* 106(6):2035–2040.
10. Zhang D, Snyder AZ, Shimony JS, Fox MD, Raichle ME (2010) Noninvasive functional and structural connectivity mapping of the human thalamocortical system. *Cereb Cortex* 20(5):1187–1194.
11. Uddin LQ, et al. (2010) Dissociable connectivity within human angular gyrus and intraparietal sulcus: Evidence from functional and structural connectivity. *Cereb Cortex* 20(11):2636–2646.
12. van den Heuvel MP, Mandl RCW, Kahn RS, Hulshoff Pol HE (2009) Functionally linked resting-state networks reflect the underlying structural connectivity architecture of the human brain. *Hum Brain Mapp* 30(10):3127–3141.
13. Saygin ZM, et al. (2012) Anatomical connectivity patterns predict face selectivity in the fusiform gyrus. *Nat Neurosci* 15(2):321–327.
14. Tzourio-Mazoyer N, et al. (2002) Automated anatomical labeling of activations in SPM using a macroscopic anatomical parcellation of the MNI MRI single-subject brain. *Neuroimage* 15(1):273–289.
15. Raichle ME, Mintun MA (2006) Brain work and brain imaging. *Annu Rev Neurosci* 29: 449–476.
16. Bassett DS, Brown JA, Deshpande V, Carlson JM, Grafton ST (2011) Conserved and variable architecture of human white matter connectivity. *Neuroimage* 54(2):1262–1279.
17. Vaishnavi SN, et al. (2010) Regional aerobic glycolysis in the human brain. *Proc Natl Acad Sci USA* 107(41):17757–17762.
18. Wedeen VJ, et al. (2012) The geometric structure of the brain fiber pathways. *Science* 335(6076):1628–1634.
19. Bassett DS, Meyer-Lindenberg A, Achard S, Duke T, Bullmore E (2006) Adaptive reconfiguration of fractal small-world human brain functional networks. *Proc Natl Acad Sci USA* 103(51):19518–19523.
20. Senden M, Goebel R, Deco G (2012) Structural connectivity allows for multi-threading during rest: The structure of the cortex leads to efficient alternation between resting state exploratory behavior and default mode processing. *Neuroimage* 60(4):2274–2284.
21. Heinze HJ, et al. (1994) Combined spatial and temporal imaging of brain activity during visual selective attention in humans. *Nature* 372(6506):543–546.
22. Fu S, Greenwood PM, Parasuraman R (2005) Brain mechanisms of involuntary visuospatial attention: An event-related potential study. *Hum Brain Mapp* 25(4):378–390.
23. Burianova H, Grady CL (2007) Common and unique neural activations in autobiographical, episodic, and semantic retrieval. *J Cogn Neurosci* 19(9):1520–1534.
24. Martin A, Chao LL (2001) Semantic memory and the brain: Structure and processes. *Curr Opin Neurobiol* 11(2):194–201.
25. Repovš G, Barch DM (2012) Working memory related brain network connectivity in individuals with schizophrenia and their siblings. *Front Hum Neurosci* 6(137):1–15.
26. Tyszka JM, Kennedy DP, Adolphs R, Paul LK (2011) Intact bilateral resting-state networks in the absence of the corpus callosum. *J Neurosci* 31(42):15154–15162.
27. Uddin LQ, Supekar KS, Ryali S, Menon V (2011) Dynamic reconfiguration of structural and functional connectivity across core neurocognitive brain networks with development. *J Neurosci* 31(50):18578–18589.
28. Supekar K, Musen M, Menon V (2009) Development of large-scale functional brain networks in children. *PLoS Biol* 7(7):e1000157.
29. Wang L, Li Y, Metzak P, He Y, Woodward TS (2010) Age-related changes in topological patterns of large-scale brain functional networks during memory encoding and recognition. *Neuroimage* 50(3):862–872.
30. Chen NK, Chou YH, Song AW, Madden DJ (2009) Measurement of spontaneous signal fluctuations in fMRI: Adult age differences in intrinsic functional connectivity. *Brain Struct Funct* 213(6):571–585.
31. Cabeza R (2002) Hemispheric asymmetry reduction in older adults: The HAROLD model. *Psychol Aging* 17(1):85–100.
32. Davis SW, Kragel JE, Madden DJ, Cabeza R (2012) The architecture of cross-hemispheric communication in the aging brain: Linking behavior to functional and structural connectivity. *Cereb Cortex* 22(1):232–242.
33. Waites AB, Briellmann RS, Saling MM, Abbott DF, Jackson GD (2006) Functional connectivity networks are disrupted in left temporal lobe epilepsy. *Ann Neurol* 59(2):335–343.
34. Monk CS, et al. (2009) Abnormalities of intrinsic functional connectivity in autism spectrum disorders. *Neuroimage* 47(2):764–772.
35. Zhang Z, et al. (2011) Altered functional-structural coupling of large-scale brain networks in idiopathic generalized epilepsy. *Brain* 134(Pt 10):2912–2928.
36. Sharp DJ, et al. (2011) Default mode network functional and structural connectivity after traumatic brain injury. *Brain* 134(Pt 8):2233–2247.
37. Zhu Q, Zhang J, Luo YLL, Dilks DD, Liu J (2011) Resting-state neural activity across face-selective cortical regions is behaviorally relevant. *J Neurosci* 31(28):10323–10330.
38. Prado J, Carp J, Weissman DH (2011) Variations of response time in a selective attention task are linked to variations of functional connectivity in the attentional network. *Neuroimage* 54(1):541–549.
39. Parker GJ, Alexander DC (2003) Probabilistic Monte Carlo based mapping of cerebral connections utilising whole-brain crossing fibre information. *Inf Process Med Imaging* 18:684–695.
40. Munier D, Lambiotte R, Fornito A, Ersche KD, Bullmore ET (2009) Hierarchical modularity in human brain functional networks. *Front Neuroinform* 3(37):1–12.
41. Bullmore E, Sporns O (2009) Complex brain networks: Graph theoretical analysis of structural and functional systems. *Nat Rev Neurosci* 10(3):186–198.
42. Friston KJ, et al. (1997) Psychophysiological and modulatory interactions in neuroimaging. *Neuroimage* 6(3):218–229.
43. Attwell D, Laughlin SB (2001) An energy budget for signaling in the grey matter of the brain. *J Cereb Blood Flow Metab* 21(10):1133–1145.
44. Bassett DS, et al. (2010) Efficient physical embedding of topologically complex information processing networks in brains and computer circuits. *PLOS Comput Biol* 6(4):e1000748.
45. Kaiser M, Hilgetag CC (2006) Nonoptimal component placement, but short processing paths, due to long-distance projections in neural systems. *PLOS Comput Biol* 2(7):e95.
46. Chen BL, Hall DH, Chklovskii DB (2006) Wiring optimization can relate neuronal structure and function. *Proc Natl Acad Sci USA* 103(12):4723–4728.